A Methodology to Discriminate Between Hydroxyl Radical-induced Processes and Direct Charge-transfer Reactions in Heterogeneous Photocatalysis

Stefano Bertinetti[1], Marco Minella[1], Francesco Barsotti[1], Valter Maurino[1], Claudio Minero[1], Emrah Özensoy[2], Davide Vione*[,1]

[1]Dipartimento di Chimica, Università di Torino, Via P. Giuria 5, 10125 Torino, Italy
[2]Department of Chemistry, Bilkent University, 06800 Ankara, Turkey

Abstract:

A method to assess the ability of a photocatalyst to induce reactions with free or trapped hydroxyl radicals versus direct charge-transfer processes is here proposed, based on the use of phenol and 2-hydroxybenzoic acid (salicylic acid) as test substrates. The rationale is that phenol degradation would be preferentially (although not exclusively) induced by hydroxyl radicals, while salicylic acid would mainly undergo direct charge-transfer oxidation. The use of t-butanol as selective $^{\bullet}$OH scavenger is helpful to understand how much each substrate is a selective indicator of the intended reaction pathway in the presence of a given semiconductor oxide. Phenol and salicylic acid should be used at low concentration (e.g. 25 μmol L^{-1}) to limit the occurrence of the back-reactions, the importance of which can be highlighted by using higher initial concentration values (e.g. 1 mmol L^{-1}). The method was optimized with the well-studied photocatalysts Evonik P25 and Wackherr's "Oxyde de titane standard", and it was then applied to study the behavior of two TiO_2/Al_2O_3 binary oxide systems (where TiO_2 occurs as a mixture of anatase and rutile). The latter photocatalysts were poorly efficient toward the degradation of phenol, but they performed better with salicylic acid. These findings, which are coherent with the results of t-butanol addition, suggest that the two binary oxide systems would induce charge-transfer rather than $^{\bullet}$OH reactions.

Keywords: heterogeneous photocatalysis; direct charge-transfer; hydroxylation; TiO_2/Al_2O_3 binary oxides.

Introduction

TiO_2-based photocatalysis is a promising advanced oxidation process for the abatement of pollutants in the water and gaseous phases. Its working principle is based on radiation absorption by the semiconductor oxide: if an incoming photon has higher energy than the semiconductor's energy gap ($h\nu \geq E_g$), it promotes an electron from the valence to the conduction band leaving a hole in the valence band. Electrons and holes can recombine in the oxide bulk, thereby dissipating the absorbed energy, or they can migrate to the semiconductor surface to be trapped by surface and sub-surface groups (1, 2). Valentin and Selloni (3) demonstrated that the trapped energy of the photo-generated carriers is higher at the surface than in the bulk, from which it follows that it is energetically favorable for the photogenerated electron/hole couples to move from the bulk to the surface. Trapped electrons can be scavenged by dissolved oxygen or other oxidizing species (4, 5), but they can also be involved in the reduction (e.g. reductive dehalogenation) of some persistent xenobiotics (6). The reaction between electrons and oxygen would ultimately lead to free hydroxyl radicals that behave as strong oxidizing agents (7). There has been controversy about the nature and reactivity of (sub)surface trapped holes (7, 8) but, from the point of view of the oxidative photo-degradation mechanism, TiO_2 can induce two different kinds of processes: *(i)* direct electron-transfer (DET) oxidation of substrates interacting with the oxide surface (e.g. surface chemisorbed substrates and/or surface physisorbed species with their hydration sphere; in the first case the mechanism is identified as inner-sphere DET, in the latter as outer-sphere DET), and *(ii)* reactions induced by free or trapped hydroxyl radicals (e.g. hydrogen abstraction or OH group addition, the latter being more likely with aromatics) (9-13). Hereafter, processes induced by free or trapped $^{\bullet}$OH (free and trapped species are particularly hard to be differentiated) will be called $^{\bullet}$OH-like induced reactions. The actual degradation pathway followed by a xenobiotic compound may affect the formation of harmless or toxic intermediates and may have

*Corresponding author; E-mail address: davide.vione@unito.it

implications for the final mineralization (19-21). Therefore, it is important to characterize the ability of a photocatalyst to favor •OH-like induced or charge-transfer (DET) reactions. A peculiar point related to the two possible oxidative mechanisms that operate under photocatalytic conditions (•OH-like induced reactions vs. DET) is that they may sometimes promote the formation of the same by-products, as observed with arenes or with the spin trapping reagent DMPO (13, 17). Therefore, it may be complicated to differentiate between the two processes when looking at the transformation intermediates.

From the comparison of the by-products detected in the photocatalytic degradation of hydroxylated aromatics or of anisoles, Jenks and coworkers proposed that the ring opening observed on ortho-substituted dihydroxyaromatic rings (strongly anchored at the TiO_2 surface) is promoted by DET oxidation, while ring hydroxylation, HO substitution and alkyl group transformation is initiated by •OH-like induced reactions (18, 19). Similar conclusions were obtained by Cermenati and coworkers, who reported the formation of different quinoline and haloquinoline by-products in the case of DET or •OH-like induced oxidation (20, 21). For a further discussion on the degradation pathways promoted by DET and/or •OH-like induced reactions with different classes of compounds, we suggest a recent review (13).

The mechanisms that are operational during the photocatalytic processes are related to both the nature of the investigated substrate and the features of the photocatalyst employed. Different crystallographic exposed phases can for instance promote specific reductive or oxidative paths (22, 23) and, consequently, the ratio between the extension of the main crystallographic phases could be a feature to be optimized to reach high photocatalytic efficiencies. The extensive study of Ryu and Choi (24) regarding the comparison of the reaction rates of 19 different substrates in the presence of different pristine and modified photocatalysts, emphasized the marked selectivity of some photocatalysts toward specific substrates and, consequently, a different ability to promote the degradation of substrates through different mechanisms. Furthermore, the role of the surface properties is essential in the definition of the photocatalytic reaction pathways. As an example, some of us demonstrated that the very defective surface of the Evonik P25 TiO_2 is effective in inducing the DET oxidation of glycerol. In contrast, truncated bipyramidal TiO_2 anatase nanoparticles that mainly expose smooth surfaces with a low density of surface defects mainly induce •OH-like oxidation (25). For presumably similar reasons, TiO_2 P25 is more effective than anatase in inducing the reductive DET decomposition of H_2O_2 (26).

Interestingly, an increment of the role of •OH-like induced with respect to DET processes was reported as a consequence of the fluorination of the TiO_2 surface (27, 28). This effect is more crucial for those catalysts like P25, the reactivity of which is dominated by surface defectivity, because the very reactive -OH groups located at the corner/edges are more prone to be substituted with redox-inert fluoride ions (29). Furthermore, Enríquez and coworkers (30) and Agrios and Pichat (31) reported that the relative importance of the DET vs. •OH-like induced pathways in oxidative transformation with UV-irradiated TiO_2 is strongly affected by the surface properties. Catalysts sintered at different time and temperature (and thus with a different degree of crystallinity and defect density) promote efficient decarboxylation and ring opening of substrates (e.g. pyridine) by direct hole transfer, while •OH-like induced processes prevail at lower sintering temperature. These considerations underline the importance of finding a method to discriminate among the different photocatalytic degradation pathways.

A popular way to assess the production of free or trapped hydroxyl radicals by irradiated TiO_2 is the transformation of terephthalic acid (TA) into the fluorescent compound 2-hydroxyterephthalic acid (TAOH) (32, 33). However, this technique only gives insight into •OH-like induced processes and it is silent as far as DET is concerned. Moreover, it might suffer from problems related to the formation of different compounds at different TA concentration values. Indeed, TA at low concentration has been shown to mainly produce 4-hydroxybenzoic acid, while TAOH formation has only been observed at mmol L^{-1} initial concentration levels of TA (34). Such a concentration effect in photocatalysis might suggest the interplay of different processes, involving for instance not only •OH-like induced vs. DET oxidation but also the possible occurrence of back reactions. The latter can occur because oxidizing and reducing species (i.e., trapped holes and electrons, respectively) are simultaneously present at the oxide surface. Therefore, a partially oxidized substrate (e.g. after reaction with •OH, free or adsorbed at the surface, or with a hole), if it is still present at or near the surface and if the process is thermodynamically allowed, can react with a trapped electron to yield back the starting compound (see reactions 1-4, where S is a generic substrate) (35). A parallel but inverse phenomenon can take place with partially reduced compounds.

$$S + {}^{\bullet}OH \rightarrow S^{\bullet}\text{-}OH \quad (1)$$

$$S + h^{+} \rightarrow S^{+\bullet} \quad (2)$$

$$S^{\bullet}\text{-}OH + e^{-} \rightarrow S + OH^{-} \quad (3)$$

$$S^{+\bullet} + e^{-} \rightarrow S \quad (4)$$

Although the back reactions may be more important for substrates undergoing DET transformation upon interaction with the photocatalyst surface, there is evidence that the photocatalytic reactions do not occur very far from the surface of the semiconductor oxide (36). Therefore, also the intermediates of the $^{\bullet}$OH-like induced processes (e.g. $S^{\bullet}$-OH in the previous reaction scheme) could occur sufficiently near the surface as to undergo back-reduction (reaction 3).

There is evidence that the back reactions are favored at elevated substrate levels, which accounts for the occurrence of maxima in photocatalytic degradation rates as a function of substrate concentration (25, 35-39). In the absence of back reactions, an increase in substrate concentration [S] at constant light intensity (that is, at equal generation rate of reactive species) would enhance the consumption of h^{+} and/or $^{\bullet}$OH and, therefore, decrease their steady-state concentration. As a consequence, the degradation rate of S would increase with [S] up to a plateau, where all the oxidizing species are consumed by S degradation (in this case, there would be negligible h^{+}-e^{-} recombination at the semiconductor surface). In the presence of back reactions at low [S], the partially oxidized species (e.g. $S^{+\bullet}$) could react with either h^{+} to be further oxidized or with e^{-} to give back S (back reaction). The latter process decreases the degradation rate compared to the case of no back reactions. If [S] is high, the consumption of h^{+} by S reduces the steady-state concentration of the oxidizing species on the semiconductor surface. The oxidation reaction between $S^{+\bullet}$ and h^{+} is thus disfavored, which in turn favors the back reaction with e^{-}. The steady-state concentration of the latter is in fact almost independent of the substrate concentration, because e^{-} mainly undergo scavenging by O_2 to approximately the same extent at any [S]. Because of the back reactions, when [S] increases, a growing fraction of the partially transformed radical species $S^{+\bullet}$ would give back the initial substrate. In other words, the relative importance of the back reactions increases with increasing [S]. If one considers that a plateau trend of the degradation rate with increasing [S] is expected without back reactions, a growing importance of the latter with increasing [S] accounts for the trend with a maximum of the degradation rates as a function of [S] (35).

Coming back to the use of TA as $^{\bullet}$OH probe in photocatalysis, the detection of TAOH requires the use of TA at mmol L^{-1} levels, where back reactions are strongly operational with many aromatic substrates (37), thereby introducing a considerable complication. In fact, one would observe the results of a mixed process where the shift from 4-hydroxybenzoic acid to TAOH could depend on the actual reaction pathways ($^{\bullet}$OH-like induced vs. DET, namely the processes one wants to highlight) and/or on the combination between direct and back reactions, which is a confounding factor. Similar problems would arise whenever one looks at the reaction intermediates to understand the reaction pathway(s).

There is literature evidence that different photocatalysts can induce $^{\bullet}$OH-like processes and DET to a different extent (21, 40), and that aromatic compounds such as phenol, benzoic acid and salicylic acid undergo preferential reaction pathways under photocatalytic conditions (37, 41). If confirmed, this issue could be an advantage because it would imply the monitoring of the primary substrate that, differently from the intermediates, enables very low concentration values to be employed. When the initial concentration of a substrate is low, the importance of the back reactions can be minimized (35-38).

The aim of the present paper is to set up a methodology to assess the ability of a photocatalyst to favor $^{\bullet}$OH-like induced or DET reactions, based on the degradation of model substrates (phenol, benzoic and salicylic acid). The test conditions were set up using easily available and well known commercial TiO_2 specimens, and the optimized methodology was then applied to study the behavior of other photocatalysts synthesized on purpose. The TiO_2 optical properties were also taken into account, because they could be important in controlling the photocatalytic activity of a given semiconductor oxide.

Experimental

Reagents and Materials

Phenol (PhOH, purity grade 99%), benzoic acid (HBz, 99.5%), salicylic acid (HSal, 99%), t-butanol (Chromasolv), $HClO_4$ (70%) and NaOH (98%) were purchased from Aldrich, methanol (gradient grade) from Carlo Erba (Cornaredo, Italy). The TiO_2 Evonik P25 (80% anatase, 20% rutile) was a gift by Evonik (previously Degussa), the TiO_2 Wackherr "Oxyde de titane standard" (anatase) was a gift by Les Colorants Wackherr (Saint-Ouen-l'Aumône, France). The methods of synthesis of P1 and P2 are reported in (42), together with an in-depth characterization of their physico-chemical properties. They consist of TiO_2/Al_2O_3

binary oxide systems, where TiO_2 occurs as a mixture of anatase and rutile. P1 and P2 resulted very effective as NO oxidation photocatalysts in gas-solid systems (42), thus it was thought interesting to test whether they also cause increased rates with respect to pristine TiO_2 in aqueous systems. The photocatalyst aqueous suspensions were prepared by ultrasonication, using a Branson 2200 water bath.

Irradiation Experiments

The solutions or suspensions to be irradiated (total volume 5 mL) were placed in cylindrical Pyrex glass cells and magnetically stirred during irradiation. The latter was carried out under a lamp Philips TLK 40W/05, with an integrated irradiance of 25±1 W m^{-2} at 300-400 nm and maximum emission at 365 nm (therefore, the lamp radiation can activate the band-to-band transition in TiO_2-based materials). This lamp has minor emission in the visible range (10±1 W m^{-2} at 400-800 nm). The UV-Vis lamp irradiance was measured with an Ocean Optics USB2000+UV-VIS CCD spectrophotometer, equipped with a 400 μm fiber optics (30 cm length) with a cosine corrector (Ocean Optics, CC-3-UV-T, optical diffuser in PTFE, wavelength range 200-2500 nm, outer diameter 6.35 mm, Field of View 180°). The spectrophotometer was calibrated with an Ocean Optics DH-2000-CAL Deuterium-Halogen Light Source, emitting in the UV-Vis-NIR and calibrated by the vendor for absolute irradiance measurements.

After the scheduled irradiation time, the cells were withdrawn from the lamp and the suspensions were filtered on Millex PVDF filter membranes (Millipore, pore diameter 0.45 μm). The filtered liquid phase was subject to further characterization.

Analytical Determinations

The time evolution of PhOH, HBz and HSal was monitored on the solutions obtained after filtration, using a High Performance Liquid Chromatograph equipped with a Diode Array Detector (HPLC-DAD). It was used a VWR-Hitachi Elite LaChrom instrument, equipped with L-2130 quaternary pump for low-pressure gradients (with Duratec external degassing unit), L-2200 autosampler, L-2300 column oven (kept at 40 °C) and L-2455 DAD detector. The column used was a Merck LiChroCART RP-18 (125 mm × 4 mm × 5 μm), with 60 μL injection volume and a flow rate of 1.0 mL min^{-1}. All samples were eluted with isocratic mixtures of methanol (A) and aqueous H_3PO_4 (B, pH 2.8); PhOH was eluted with 30% A (detection wavelength 210 nm, retention time 5.1 min), HBz with 40% A (225 nm, 5.4 min) and HSal with 30% A (220 nm, 9.8 min). The column dead time was 1.3 min.

Attenuation spectra of photocatalyst suspensions (0.05 g L^{-1} loading) were taken with a Varian Cary 100 Scan double-beam, UV-vis spectrophotometer, using Hellma quartz cuvettes with 1 cm optical path length. Particle diameters were determined by Dynamic Light Scattering (DLS). The used instrument was an ALV-NIBS High Performance Particle Sizer (ALV GmbH, Germany), equipped with a Ne-He laser and with an ALV-500 multiple tau digital correlator. Samples were suspended in ultra-pure water and analyzed by recording the intensity of the scattered light at an angle of 173° for 30 seconds at 25 °C.

The adsorption of the substrates on the photocatalysts was tested by comparing the substrate concentration in a solution with pure water, with that in the liquid phase obtained after filtration of a photocatalyst suspension at the same total initial substrate. Measurable adsorption in a wide range of concentration values could be excluded at 0.2 g L^{-1} photocatalyst loading, but adsorption was significant in the presence of 25 μmol L^{-1} HSal and 2 or 5 g L^{-1} TiO_2 loading. In this case, it was assumed that the amount of adsorbed HSal would be proportional to the residual concentration in the liquid phase, which is reasonable when the substrate concentration is low (38). By so doing, the aqueous-phase HSal concentration would also be proportional to the total HSal concentration occurring in the reaction system (dissolved + adsorbed, and referred to the total volume) (38).

Kinetic Data Treatment

The photodegradation of the studied substrates followed pseudo-first order kinetics. The time trend of the concentration values was fitted with a pseudo-first order equation of the form $C_t = C_o \exp(-k\,t)$, where C_t is the substrate concentration at the time t, C_o the initial concentration, and k the pseudo-first order degradation rate constant. The initial degradation rate was $R = k\,C_o$. The main source of uncertainty was related to the determination of k, thus the reported uncertainty on R mainly depended on the k uncertainty (goodness of the fit of the experimental data with the theoretical curve, representing intra-series variability). The reproducibility of repeated runs (inter-series variability) was around 10-15%.

Results and Discussion

This work is organized into two sections. In the first one, substrate and reaction conditions were optimized to highlight the role of •OH-like induced reactions vs. DET processes in the photoreactivity of a given TiO_2 specimen. This part of the work was carried

out on two well-studied varieties of TiO_2, namely Evonik P25 (hereafter P25) and Wackherr's "Oxyde de titane standard" (hereafter W). In the second section, the optimized conditions were used to study the photodegradation features of the test photocatalysts (P1 and P2).

Choice of Model Substrates and Reaction Conditions

The chosen standard TiO_2 loading was 0.2 g L^{-1}, a reasonable value that affords sufficiently fast degradation while limiting the potential problems connected to substrate adsorption on the photocatalyst and to light scattering (43, 44). Other important reaction parameters are pH and substrate concentration. The pH value is important because it affects the interaction between the substrate and TiO_2 (involving negatively charged species in the case of HBz and HSal), as well as the acid/base speciation of the TiO_2 hydroxyl groups and the reactivity of the photo-formed oxidizing species at the photocatalyst surface (45, 46). Note that the Fermi level position of TiO_2 and, consequently, the oxidizing properties of the photoproduced species on irradiated TiO_2 are strongly related to both pH and the nature of the other ions in solution, which can strongly modify the double-layer structure of the solid/electrolyte interface (47). In the case of HSal and HBz, the charge interactions between positively charged TiO_2 and the partially occurring negative substrates would be maximized at pH ~ 3. Such interactions are potentially favorable to the DET process (37, 41). The issue of charge interaction with the TiO_2 surface does not apply to phenol, but the pH effect on phenol degradation was checked for comparison purposes.

The substrate concentration is important because of the possible occurrence of the back reactions. These processes may cause a trend with a maximum of the degradation rates with increasing substrate concentration (35-38), thus it is important to highlight the role of the back reactions when measuring the photocatalytic degradation rates.

The pH trend of the degradation rates of phenol (PhOH), benzoic acid (HBz) and salicylic acid (HSal) is reported in Figure 1, in the presence of the P25 (1a) and W (1b) TiO_2 specimens. In all the cases the degradation rates increased with increasing pH, but the pH trend was quite limited for PhOH and HBz with P25. PhOH and HBz also showed similar degradation rates and pH trends with the same photocatalyst (P25 or W), which might imply the occurrence of comparable reaction pathways. In the case of HBz and HSal, operation at pH 3 would maximize the interaction

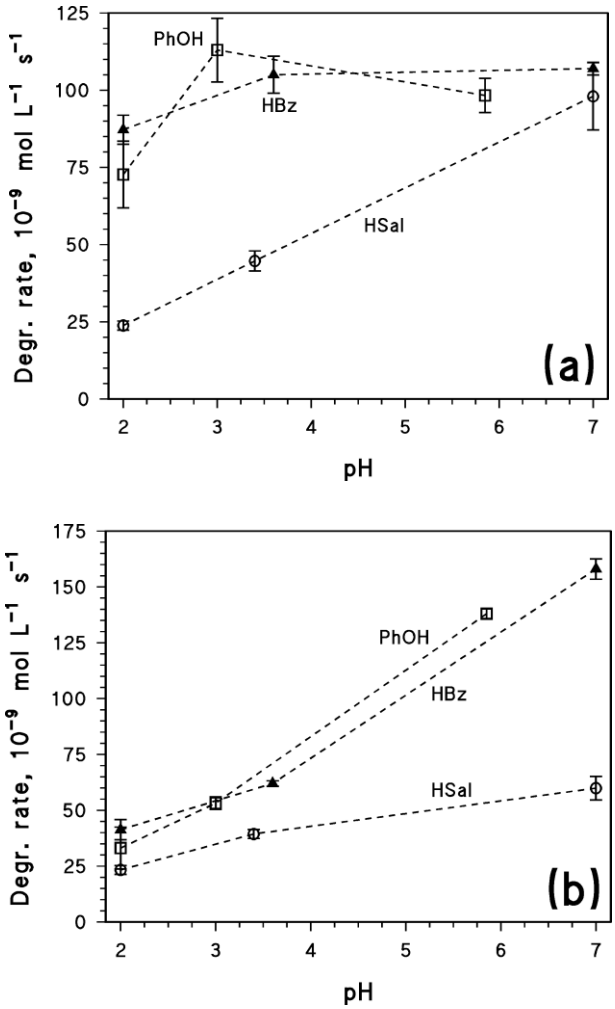

Figure 1. Trend with pH of the photocatalytic degradation rates of PhOH, HBz and HSal (initial concentration 0.5 mmol L^{-1}), in the presence of 0.2 g L^{-1} TiO_2 P25 **(a)** and W **(b)**. When needed, the solution pH was adjusted with $HClO_4$ or NaOH. The error bars represent σ-level uncertainties.

with the TiO_2 surface and, hence, the occurrence of DET. In the case of PhOH there are two arguments against the choice of ~neutral pH conditions: *(i)* they would imply the testing of HBz, HSal and PhOH at different pH values, and *(ii)* comparability issues might arise, because PhOH degradation showed for instance very different pH trends with P25 and W. Furthermore, in ~neutral systems a drift of the pH during the irradiation experiments could be possible as a consequence of the low buffer potential of the solutions, thereby changing the experimental conditions. For the reported reasons, all the subsequent experiments were carried out at pH 3.

The effect of the addition of t-butanol was studied to check the reliability of PhOH, HBz and HSal as selective substrates to understand the photoreaction pathways. The t-butanol is a rather selective scavenger of hydroxyl radicals in photocatalysis (either trapped

at the photocatalyst surface or free in the solution bulk), and it undergoes more limited charge-transfer processes compared to other alcohols (48-50). A different t-butanol effect should thus be expected with substrates undergoing different photodegradation pathways. The results of the addition of t-butanol (initial concentration 10 mmol L^{-1}) on the degradation rates of the studied substrates (at 0.25 mmol L^{-1} initial concentration) are reported in Figure 2 for P25 (2a) and W (2b). It was used a 40:1 concentration ratio between t-butanol and the substrates, because the second-order reaction rate constants with •OH are about an order of magnitude higher for PhOH, HBz and HSal compared to the alcohol (48). Moreover, it was previously verified that t-butanol did not modify significantly the adsorption properties of the aromatic substrates onto TiO_2, at the used concentration values. The comparison of the degradation rates with and without t-butanol suggests that the alcohol effect was not substantial in the case of P25. In fact, the addition of t-butanol decreased the PhOH and HSal degradation rates by ~40%, and that of HBz by ~30%. More marked differences could be observed in the case of W: the addition of t-butanol decreased the degradation rates by 70-75% for PhOH and HBz, and by ~20% for HSal. The W results can be explained under the hypothesis that the majority of PhOH and HBz degradation took place by •OH-like induced processes, while HSal mainly reacted through DET. In contrast, in the case of P25 one would conclude that the degradation of the three substrates would be a combination of •OH-like induced reactions and DET. This is in agreement with the high degree of defectivity of the surface of P25. The low-coordination sites at the P25 surface are often specific adsorption sites (29), where DET processes are favored over •OH-like induced reactions that instead dominate on the extended facets (25). On the contrary, the surface of the larger W nanoparticles is more regular and favors the •OH-like induced reactions (21).

The trends of the degradation rates as a function of substrate concentration for P25 and W are reported in Figure 3 for PhOH (3a), HBz (3b) and HSal (3c). In all the cases one can observe a rate decrease at elevated substrate, coherently with a significant occurrence of the back reactions (35-38). For higher substrate concentration values than those corresponding to the rate maxima, substrate degradation would measure both the occurrence of •OH-like/DET processes and the role of the back reactions, thereby underlining a mixed scenario. To get more specific insights into the primary photodegradation pathways, low substrate concentration values should thus be selected.

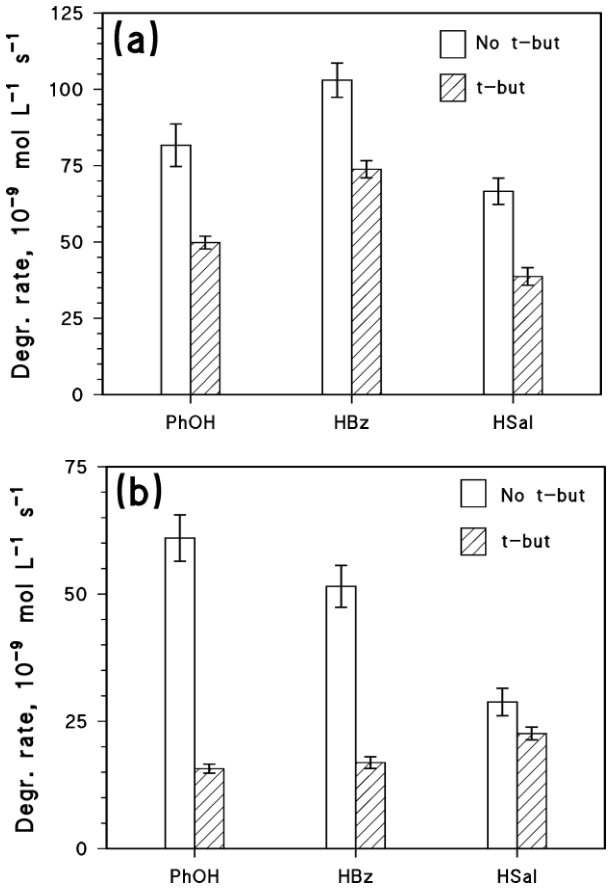

Figure 2. Photocatalytic degradation rates of PhOH, HBz and HSal (initial concentration 0.25 mmol L^{-1}), with and without addition of 10 mmol L^{-1} t-butanol, in the presence of 0.2 g L^{-1} TiO_2 P25 **(a)** and W **(b)** at pH 3, adjusted with $HClO_4$. The error bars represent σ-level uncertainties.

The runs previously reported suggest that HSal would be less affected than HBz by •OH-like induced reactions, thereby favoring the use of HSal and PhOH as test substrates. On this basis, HSal degradation would be used to gauge the DET processes and PhOH the •OH-like induced ones. The relative ability of a photocatalyst to induce the degradation of the two substrates could thus be an index of its tendency to favor DET vs. •OH-like induced reactions. The reaction conditions were optimized in the presence of P25 and W, the availability of which in reasonably large amount allowed several tests to be carried out. The new photocatalysts to be tested were available in more limited amount, which placed a restriction on the number of runs that could be carried out. Therefore, the experiments aimed at characterizing the photocatalytic activity of P1 and P2 were performed with PhOH and HSal at pH 3, using substrate concentrations of 25 μmol L^{-1} (to limit back reactions) and 1 mmol L^{-1} (to get insight into the possible back-reaction effects). The standard TiO_2 loading was 0.2 g L^{-1}, but

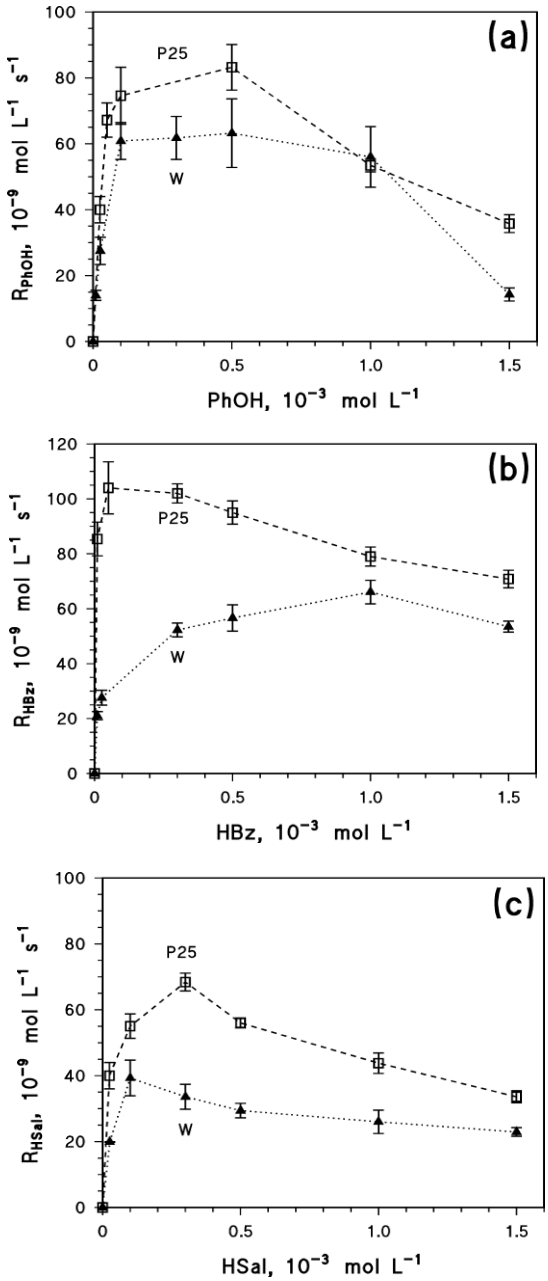

Figure 3. Initial photocatalytic degradation rates of PhOH **(a)**, HBz **(b)** and HSal **(c)** as a function of substrate concentration, in the presence of 0.2 g L^{-1} TiO_2 (P25 or W) at pH 3, adjusted with $HClO_4$. The error bars represent σ-level uncertainties.

different loading values were also used to highlight the effects of the peculiar optical properties of the new photocatalysts.

Test of the Reactivity of the New Photocatalysts (P1 and P2)

Optical Properties

The attenuation spectra (absorption + scattering) of the four TiO_2 specimens considered in this work are reported in Figure 4 (the photocatalyst loading was

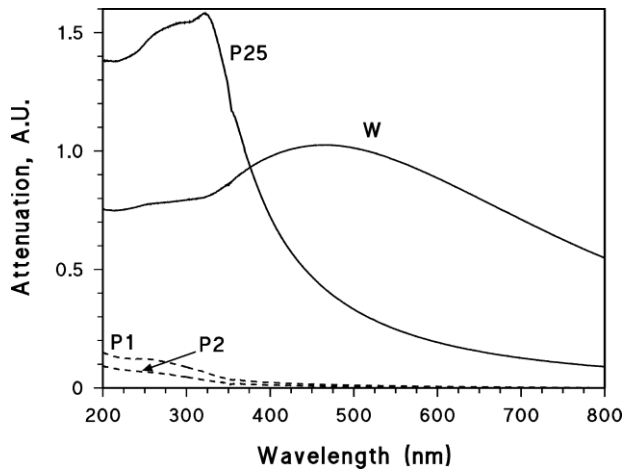

Figure 4. Optical attenuation spectra of the four tested photocatalysts, at 50 mg L^{-1} loading and with an optical path length of 1 cm.

50 mg L^{-1} in all the cases). There is higher optical attenuation of P25 compared to W below 400 nm, which is consistent with previous reports and is mainly due to higher scattering by P25 (note that the absorption of TiO_2 P25 is limited compared to scattering, at least above 300 nm (37, 51)). The different optical properties between P25 and W are mainly due to different particle size, with W having considerably larger particles than P25 (50 nm average radius for P25, compared to 150-160 nm for W). Because scattering decreases the efficiency by which a photocatalyst can use the incoming radiation (51), lower radiation scattering can offset (to a variable degree depending on substrate and reaction conditions) the lower surface area of larger particles, as far as photocatalytic activity is concerned (12, 21, 37, 38, 52). The radiation attenuation of the samples P1 and P2 is remarkably low, which suggests a very low degree of radiation scattering. The low scattering would be connected partially to particle size (P2 has very large particles of ~1 μm diameter, but the particle size of P1 is comparable to that of W), and partially to the fact that alumina, which makes up a remarkable mass percentage of both P1 and P2, poorly scatters radiation as a consequence of its low refraction index compared to TiO_2 (n_{TiO_2} = 2.6, $n_{Al_2O_3}$ = 1.8) (53, 54). This feature makes P1 and P2 potentially interesting photocatalysts at high loading values, where the photocatalytic activity is usually severely limited by radiation scattering (55).

Photocatalytic Activity

The photoactivity of P1 and P2 was tested towards the degradation rates of phenol (R_{PhOH}) and HSal (R_{HSal}). The two substrates were tested at different

concentration values (25 μmol L^{-1} and 1 mmol L^{-1}), to get some insight into the possible importance of the back reactions. The photocatalysts P1 and P2 were scarcely effective in degrading PhOH. Irradiated P1 at 0.2 g L^{-1} loading induced the degradation of 25 μmol L^{-1} PhOH with R_{PhOH} = (7.3±1.7)·10^{-10} mol L^{-1} s^{-1}, namely ~40 times lower than P25 under comparable conditions (and ~35 times lower than W). In the case of 1 mmol L^{-1} PhOH with 0.2 g L^{-1} P1, it was R_{PhOH} = (2.8±0.4)·10^{-9} mol L^{-1} s^{-1} (~20 times lower than P25 or W). The photocatalyst P2 performed even worse: it was R_{PhOH} = (9.8±2.4)·10^{-11} mol L^{-1} s^{-1} with 25 μmol L^{-1} PhOH (~400 and ~250 times lower than P25 and W, respectively), and R_{PhOH} = (1.8±0.6)·10^{-9} mol L^{-1} s^{-1} with 1 mmol L^{-1} PhOH (25-30 times lower than P25 or W).

The performance of P1 and P2 was a bit better toward HSal degradation. A 0.2 g L^{-1} P1 suspension induced the transformation of 25 μmol L^{-1} HSal with R_{HSal} = (5.3±0.6)·10^{-9} mol L^{-1} s^{-1} (~8 times lower than P25 and ~4 times lower than W). Moreover, 1 mmol L^{-1} HSal showed R_{HSal} = (3.8±0.2)·10^{-9} mol L^{-1} s^{-1} (~12 times lower than P25 and ~7 times lower than W under comparable conditions). Irradiated P2 with 25 μmol L^{-1} HSal gave R_{HSal} = (1.3±0.1)·10^{-9} mol L^{-1} s^{-1} (~30 and ~15 times lower than P25 and W, respectively), while in the presence of 1 mmol L^{-1} HSal it was R_{HSal} = (3.1±0.2)·10^{-9} mol L^{-1} s^{-1} (~15 and ~8 times lower than P25 and W, respectively).

The degradation of PhOH and HSal with P1 and P2, compared to P25 and W, indicates that P1 and P2 were less photoactive than the reference photocatalysts, especially towards PhOH. Based on previous discussion and literature findings (27, 41), a peculiarly low photoactivity with PhOH suggests that P1 and P2 would hardly favor •OH-like induced processes. Additional tests carried out by addition of t-butanol indicate a very small effect of the alcohol on PhOH degradation by P1 and P2, thereby suggesting that even the limited degree of the PhOH degradation would mainly take place by DET. The elevated importance of DET in the photocatalytic activity of P1 and P2 is coherent with the better results obtained with HSal degradation compared to PhOH.

The considerable role of DET in the photocatalytic activity of P1 and P2 might be connected with the elevated annealing temperature (> 700 °C) that was used to obtain the two photocatalysts (42). Indeed, annealing at high temperature might produce an extensive reconstruction of the oxide surface (56, 57) and, most notably, a decrease of the surface density of the -OH groups. In fact, the latter undergo

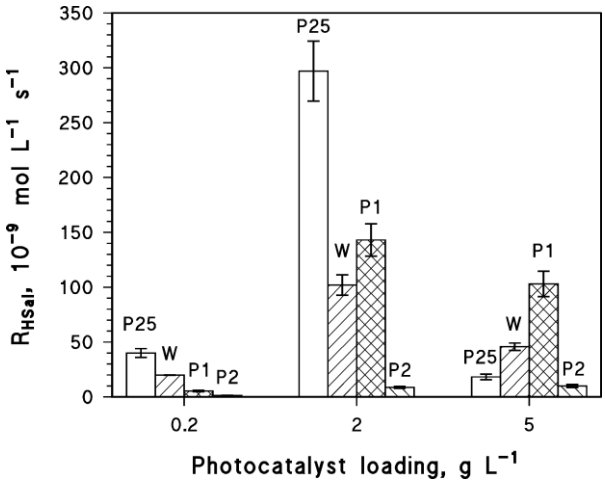

Figure 5. Photocatalytic degradation rate of 25 μmol L^{-1} HSal, in the presence of the four tested photocatalysts (P25, W, P1, P2) at different loading values. The pH of the suspensions was 3, adjusted with $HClO_4$. The error bars represent σ-level uncertainties.

recombination followed by H_2O desorption during high-temperature calcination, and a lower -OH surface density could be detrimental to •OH-like induced processes. Indeed, it has been reported that the tendency of a photocatalyst to induce •OH-like vs. DET reactions decreases with an increase in the annealing temperature (30, 31).

In the previous section it was reported that P1 and P2 showed limited scattering of radiation, which could make them effective at elevated loading. The results shown in Figure 5 compare the degradation rates of 25 μmol L^{-1} HSal at different loading values of the various photocatalysts (0.2, 2 and 5 g L^{-1}). One observes that P1 became competitive toward HSal degradation at 2 g L^{-1} loading and was the most effective photocatalyst at 5 g L^{-1}, coherently with the low radiation scattering. In the case of P1, the increase of the catalyst loading increased the reactive surface area without decreasing too much the amount of available photons that could induce the photocatalytic process. The transformation of HSal by P2, although significant at elevated loading, did not increase enough to make the process competitive with the other photocatalysts.

With the exception of P2, in the other cases the order of HSal degradation rates at 5 g L^{-1} loading (P1 > W > P25) followed the reverse order of radiation attenuation below 400 nm (P25 > W > P1, see Figure 4), in agreement with a pivotal role of the scattering in the overall attenuation coefficient. In view of practical applications, however, the use of P1 at elevated loading (e.g. 5 g L^{-1}) looks little justified considering that 2 g L^{-1} P25 was more than twice as effective (see Figure 5).

Conclusions

The use of phenol (PhOH) and salicylic acid (HSal) as test molecules, to study the photocatalytic activity of a semiconductor oxide, can provide insight into the relative importance of •OH-like induced reactions and DET processes. The two compounds provide a reasonably selective but not totally specific differentiation between the different reaction pathways, thus the additional use of t-butanol as •OH scavenger is recommended.

The commercial TiO_2 specimens P25 and W were used as reference materials, compared to which the synthesized photocatalysts P1 and P2 were much less photoactive. With reference to P25 and W, both P1 and P2 would strongly favor DET over •OH-like induced processes, as demonstrated by the faster degradation of HSal compared to PhOH, and by the effect of the addition of t-butanol. P1 and P2 showed very limited radiation scattering below 400 nm, which favors photoactivity at elevated photocatalyst loading. Indeed, P1 proved to be the photocatalyst inducing the fastest HSal degradation at a TiO_2 loading of 5 g L^{-1}.

The reported findings also suggest that the tests of photocatalytic reactivity might be poorly conclusive when carried out with a single probe molecule at only one concentration value. Suitable tests with more substrates at different concentrations can provide insight into the role of different degradation pathways (e.g. •OH-like induced reactions vs. DET), as well as the back reactions. Furthermore, in photocatalytic reaction tests it is very important to get insight into the optical properties of the studied materials, because the scattering behavior can deeply alter the degradation performance as a function of loading. Finally, the test conditions optimized in this work could be used to characterize the reactivity of other semiconductor oxides in aqueous suspension.

References

(1) Fujishima, A.; Zhang, X.T.; Tryk, D.A. *Surf. Sci. Rep*. **2008**, *63*, 515-582.

(2) Chong, M.N.; Jin, B.; Chow, C.W.K., Saint, C. *Water Res*. **2010**, *44*, 2997-3027.

(3) Valentin, C.D.; Selloni, A. *J. Phys. Chem. Lett*. **2011**, *2*, 2223-2228.

(4) Evgenidou, E.; Konstantinou, I.; Fytianos, K.; Poulios, I.; Albanis, T. *Catal. Today* **2007**, *124*, 156-162.

(5) Armakovic, S.J.; Armakovic, S.; Fincur, N.L.; Sibul, F.; Vione, D.; Setrajcic, J.P.; Abramovic, B.F. *RSC Adv*. **2015**, *5*, 54589-54604.

(6) Calza, P.; Minero, C.; Pelizzetti, E. *Environ. Sci. Technol.* **1997**, *31*, 2198-2203.

(7) Salvador, P. *J. Phys. Chem. C* **2007**, *111*, 17038-17043.

(8) Liao, H.D.; Reitberger, T. *Catalysts* **2013**, *3*, 418-443.

(9) Villarreal, T.L.; Gomez, R.; Neumann-Spallart, M.; Alonso-Vante, N.; Salvador, P. *J. Phys. Chem. B* **2004**, *108*, 15172-15181.

(10) Meichtry, J.M.; Quici, N.; Mailhot, G.; Litter, M.I. *Appl. Catal. B: Environ*. **2011**, *102*, 454-463.

(11) Meichtry, J.M.; Quici, N.; Mailhot, G.; Litter, M.I. *Appl. Catal. B: Environ*. **2011**, *102*, 555-562.

(12) Abramovic, B.; Sojic, D.; Despotovic, V.; Vione, D.; Pazzi, M.; Csanadi J. *Appl. Catal. B: Environ*. **2011**, *105*, 191-198.

(13) Jenks, W.S. In *Photocatalysis and Water Purification: From Fundamentals to Recent Applications*; Pichat, P., Ed.; Wiley-VCH: Weinheim, 2013; pp 25-51.

(14) Konstantinou, I.K.; Albanis, T.A. *Appl. Catal. B: Environ.* **2003**, *42*, 319-335.

(15) Konstantinou, I.K.; Albanis, T.A. *Appl. Catal. B: Environ*. **2004**, *49*, 1-14.

(16) Abramovic, B.; Kler, S.; Sojic, D.; Lausevic, M.; Radovic, T.; Vione, D. *J. Hazard. Mater*. **2011**, *198*, 123-132.

(17) Nosaka, Y.; Komori, S.; Yawata, K.; Hirakawa, T.; Nosaka, A.Y. *Phys. Chem. Chem. Phys*. **2003**, *5*, 47361-4735.

(18) Li, X.; Cubbage, J.W.; Jenks, W.S. *J. Org. Chem*. **1999**, *64*, 8525-8536.

(19) Li, X.; Cubbage, J.W.; Tetzlaff, T.A.; Jenks, W.S. *J. Org. Chem*. **1999**, *64*, 8509-8524.

(20) Cermenati, L.; Pichat, P.; Guillard, C.; Albini, A. *J. Phys. Chem B* **1997**, *101*, 2650-2658.

(21) Cermenati, L.; Albini, A., Pichat, P.; Guillard, C. *Res. Chem. Intermed*. **2000**, *26*, 221-234

(22) Ohno, T.; Sarukawa, K.; Matsumura, M. *New J. Chem*. **2002**, *26*, 1167-1170.

(23) Taguchi, T.; Saito, Y.; Sarukawa, K.; Ohno, T.; Matsumura, M. *New J. Chem*. **2003**, *27*, 1304-1306.

(24) Ryu, J.; Choi, W. *Environ. Sci. Technol*. **2008**, *42*, 294-300.

(25) Minero, C.; Bedini, A.; Maurino, V. *App. Catal. B: Environ*. **2012**, *128*, 135-143.

(26) Deiana, C.; Minella, M.; Tabacchi, G.; Maurino, V.; Fois, E.; Martra, G. *Phys. Chem. Chem. Phys*. **2013**, *15*, 307-315.

(27) Minero, C.; Mariella, G.; Maurino, V.; Pelizzetti, E. *Langmuir* **2000**, *16*, 2632-2641.

(28) Minero, C.; Mariella, G.; Maurino, V.; Vione, D.; Pelizzetti, E. *Langmuir* **2000**, *16*, 8964-8972.

(29) Minella, M.; Faga, M.G.; Maurino, V.; Minero, C.; Pelizzetti, E.; Coluccia, S.; Martra, G. *Langmuir* **2010**, *26*, 2521-2527.

(30) Enríquez, R.; Agrios, A. G.; Pichat, P. *Catal. Today* **2007**, *120*, 196-202.

(31) Agrios, A.G.; Pichat, P. *J. Photochem. Photobiol. A-Chem*. **2006**, *180*, 130-135.

(32) Ishibashi, K.; Fujishima, A.; Watanabe, T.; Hashimoto, K. *Electrochem. Commun*. **2000**, *2*, 207-210.

(33) Cao, J.; Luo, B.D.; Lin, H.L.; Chen, S.F. *J. Hazard. Mater*. **2011**, *190*, 700-706.

(34) Bubacz, K.; Kusiak-Nejman, E.; Tryba, B.; Morawski, A.W. *J. Photochem. Photobiol. A: Chem*. **2013**, *261*, 7-11.

(35) Minero, C. *Catal. Today* **1999**, *54*, 205-216.

(36) Minero, C.; Catozzo, F.; Pelizzetti, E. *Langmuir* **1992**, *8*, 481-486.

(37) Vione, D.; Minero, C.; Maurino, V.; Carlotti, M. E.; Picatonotto, T.; Pelizzetti, E. *Appl. Catal. B: Environ*. **2005**, *58*, 79-88.

(38) Minero, C.; Vione, D. *Appl. Catal. B: Environ*. **2006**, *67*, 257-269.

(39) Minero, C.; Maurino, V.; Vione, D. In *Photocatalysis and Water Purification: From Fundamentals to Recent Applications*; Pichat, P., Ed.; Wiley-VCH: Weinheim, 2013; pp 53-72.

(40) Maurino, V.; Bedini, A.; Minella, M.; Rubertelli, F.; Pelizzetti, E.; Minero, C. *J. Adv. Oxid. Technol*. **2008**, *11*, 184-192.

(41) Vione, D.; Picatonotto, T.; Carlotti, M.E. *J. Cosmetic Sci*. **2003**, *54*, 513-524.

(42) Polat, M.; Soylu, A.M.; Erdogan, D.A.; Erguven, H.; Vovk, E.I.; Ozensoy, E. *Catal. Today* **2015**, *241*, 25-32.

(43) Ballari, M.D.M.; Brandi, R.; Alfano, O.; Cassano, A. *Chem. Eng. J*. **2008**, *136*, 242-255.

(44) Turolla, A.; Santoro, D.; de Bruyn, J.R.; Crapulli, F.; Antonelli, M. *Water Res*. **2016**, *88*, 117-126.

(45) Stapleton, D.R.; Konstantinou, I.K.; Mantzavinos, D.; Hela, D.; Papadaki, M. *Appl. Catal. B: Environ*. **2010**, *95*, 100-109.

(46) Ahmed, S.; Rasul, M.G.; Brown, R.; Hashib, M.A. *J. Environ. Manage*. **2011**, *92*, 311-330.

(47) Minella, M.; Maurino, V.; Minero, C.; Pelizzetti, E. *J. Nanosci. Nanotechnol* **2015**, *15*, 3348-3355.

(48) Buxton, G.V.; Greenstock, C.L.; Helman, W.P.; Ross, A.B. *J. Phys. Chem. Ref. Data* **1988**, *17*, 513-886.

(49) Chabita, K.; Saha, A.; Mandal, P.C.; Bhattacharyya, S.N.; Rath, M.C.; Mukherjee, T. *Res. Chem. Intermed.* **1996**, *22*, 225-240.

(50) Zhang, Y.J.; Zhuang, Y.Y.; Wu, C.Y.; Li, S.; Ma, J. *J. Environ. Eng*. **2015**, *141*, 04014080.

(51) Cabrera, M.I.; Alfano, O.M.; Cassano, A.E. *J. Phys. Chem*. **1996**, *100*, 20043-20050.

(52) Marugan, J.; Van Grieken, R.; Alfano, O.M.; Cassano, A.E. *AICHE J*. **2006**, *52*, 2832-2843.

(53) Apetz, R.; vab Bruggen, M.P.B. *J. Am. Ceram. Soc*. **2003**, *86*, 480-486.

(54) http://refractiveindex.info/ last acces 14th January 2016.

(55) Liu, T.X.; Liu, Y.; Zhang, Z.J.; Li, F.B.; Li, X.Z. *Ind. Eng. Chem. Res*. **2011**, *50*, 7841-7848.

(56) Sun, J.; Wu, J.M. *Sci. Adv. Mater*. **2013**, *5*, 549-556.

(57) Han, Y.; Kim, H.S.; Kim, H. *J. Nanomater*. **2012**, 427453.

Received for review January 15, 2016. Revised manuscript received March 2, 2016. Accepted March 4, 2016.